

Liquid dynamics in partially crystalline glycerol

Alejandro Sanz* and Kristine Niss

IMFUFA, Department of Science and Environment,
Roskilde University, Postbox 260, DK-4000 Roskilde, Denmark

(Dated: October 14, 2016)

We present a dielectric study on the dynamics of supercooled glycerol during crystallization. We explore the transformation into a solid phase in real time by monitoring the temporal evolution of the amplitude of the dielectric signal. Neither the initial nucleation or the crystal growth influence the liquid dynamics visibly. For one of the samples studied, a tiny fraction of glycerol remained in the disordered state after the end of the transition. We examined the nature of the α relaxation in this frustrated crystal and find that it is virtually identical to the bulk dynamics. In addition to that, we have found no evidence that supercooled glycerol transforms into a peculiar phase where either a new solid amorphous state or nano-crystals dispersed in a liquid matrix are formed.

I. INTRODUCTION

One of the long standing questions in the field of condensed matter physics is what governs the liquid-to-glass transition and the concomitant dramatic slowing down of the transport quantities when supercooled liquids approach the glassy state on cooling?¹⁻³. At the glass transition temperature T_g the liquid falls out of thermodynamic equilibrium because the molecular rearrangements become so slow that *ie* the equilibrium volume and enthalpy^{4,5} cannot be reached on experimental time scales. In fact the main focus in the field is the molecular relaxation taking place in the supercooled liquid just above T_g . The main relaxation process, referred to as the α relaxation, is cooperative in nature and can be measured as a response to a wide range of external perturbations, for instance mechanical or electrical⁶. By utilizing dielectric spectroscopy methods, the α relaxation is manifested in both the real and imaginary parts of the complex dielectric permittivity as a step-like and as a maximum respectively^{7,8}. The glass-formers community has widely exploited the imaginary part of the complex dielectric permittivity because of its high sensitivity to external factors such as temperature and pressure, but also to microscopic properties of the substance such as its degree of order, physical interactions with the surroundings and geometrical confinement among others⁹⁻¹⁵.

Glycerol (propane-1,2,3-triol) is one of the most studied molecular glass-formers, principally for its extremely low tendency to crystallize^{7,16-21}. With three hydroxyl groups distributed uniformly along the aliphatic chain, glycerol molecules show very high flexibility that, together with a rich hydrogen-bonded network, allow this system to explore multitude of molecular conformations and structural fluctuations²²⁻²⁴. Since glycerol normally forms a highly stable supercooled liquid (large viscosity about melting¹⁸), little attention has been paid to its crystalline phase. Even so, one can find in the literature several works mainly focused on the high frequency dynamics of the crystalline state²⁵⁻²⁷. Nevertheless, real time investigations of its transformation into solid-like structures has recently attracted the interest of some authors^{28,29}. Inspired by previous works on the existence

of long-lived dynamic heterogeneities in supercooled glycerol, Möbious *et al.* performed real time ageing experiments above the T_g and detected the formation of a solid phase that showed a distinct mechanical performance as compared to the orthorhombic crystal²⁸. Precisely, the solid-like phase induced by the experimental protocol followed by these authors presented a value of the shear modulus two orders of magnitude lower than that of standard crystalline glycerol. In this way, Möbious and co-authors *speculated* with the existence of a glacial phase³⁰, that is, either a second amorphous phase or a frustrated crystal with a high degree of defects and disorder. Two years later, by employing time-resolved neutron scattering, Yuan and co-authors aimed to unravel the structural nature of this solid-like phase²⁹. They revealed, in agreement with one of the interpretations given by Möbious *et al.*, the formation of a crystalline lattice.

It is well established that there is an interplay between structure and dynamics on the phenomenon of crystallization^{31,32}, though the exact nature of this is not well understood. Aspects such as the existence of pre-ordered configurations in the liquid near the crystal-liquid interface, the reorganization of the liquid structure as a previous step to the formation of the crystals and spatial confinement effects imposed by the crystalline phase on the liquid dynamics, have been introduced to draw the attention about the close interrelationship between structure and dynamics in molecular liquids during crystallization^{31,33-35}.

The focus in this paper is on how the nucleation and growth steps of crystallization of glycerol, affect the dynamics of the remaining liquid. Moreover we study the dynamics of a partially disordered sample, shedding light on the putative existence of a glacial phase.

II. SAMPLE PREPARATION AND EXPERIMENTAL TOOLS

Anhydrous glycerol (≥ 99.5 % purity, Sigma-Aldrich®) was used without ulterior purification and manipulated, as much as we could, under nitrogen to avoid the uptake of ambient water. In order to carry out the present

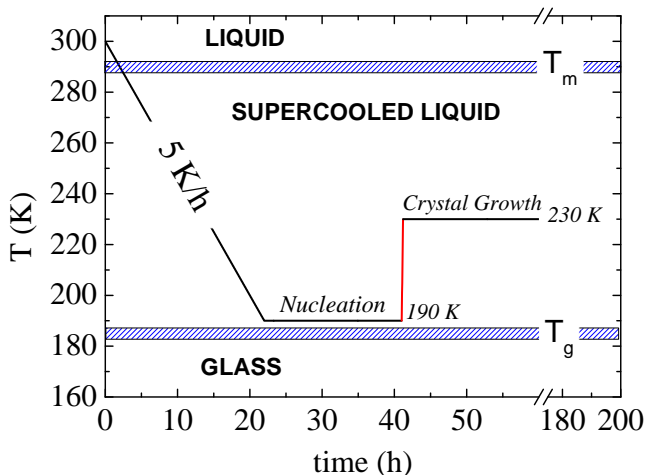


FIG. 1. Thermal protocol for inducing the transformation of liquid glycerol into the crystalline phase. Nucleation of crystalline seeds is promoted by annealing at 190 K during 19 hours. Crystal growth takes place at 230 K.

study, we utilized broadband dielectric spectroscopy, using a sample cell specially designed for this kind of measurements. It consists of two parallel metal plates, separated by a kapton[®] spacer of 0.25 mm thickness. With the purpose of insulating the sample cell electrically and also from possible water contamination, the capacitor was sealed by means of a cylindrical container made of polyether ether ketone (PEEK).

We filled the transducer with dry glycerol under nitrogen flow inside a glove bag. Once the cell was properly closed, it was transferred to the measuring cryostat. For a detailed description of the dielectric spectroscopy setup and sample environment control we refer the reader to the following publication^{36,37}.

The standard procedure we followed to induce the crystallization of supercooled glycerol consisted in the thermal protocol described in Fig. 1. We cooled down the sample from 300 K to 190 K at a cooling rate of approximately 5 K/h. Then, an isothermal annealing at 190 K was carried out. Finally, we heated up to 230 K where we monitored isothermally the dielectric signal as crystallization went by.

III. RESULTS

A. Dynamics of the fully disordered liquid

First, we examined the dynamics of the fully disordered liquid. Figure 2 shows, at selected temperatures, the frequency evolution of the complex dielectric permittivity, $\varepsilon^*(\omega) = \varepsilon'(\omega) - i\varepsilon''(\omega)$, where ω is the angular frequency, and ε' and ε'' are the real and imaginary parts respectively. The spectra were acquired on heating, after cooling the sample to the lowest temperature measured.

The maxima and the inflection points displayed in Fig. 2 correspond to the α relaxation. The location of the maximum loss for the α relaxation and the absolute values of the permittivity are in agreement with the literature^{7,20}. We described the relaxation curves with a dielectric version of the α circuit model, also known as the dielectric version of the Extended Bell (EB) model³⁸. The complex dielectric permittivity according to the α circuit model reads as follows:

$$\varepsilon^*(\omega) = \varepsilon_\infty + \frac{\Delta\varepsilon}{1 + \frac{1}{(i\omega\tau_\alpha)^{-1} + k_\alpha(i\omega\tau_\alpha)^{-\alpha}}} \quad (1)$$

Here, ε_∞ is the instantaneous or unrelaxed dielectric constant, $\Delta\varepsilon$ is the dielectric strength, τ_α is the α -relaxation time, α is the high-frequency power law³⁹ and k_α determines the broadening of the α peak.

B. Dynamics during nucleation

The main aim of this work is to shed additional light to the dynamics-structure relationships during the transformation of liquid glycerol into an ordered solid phase. A fresh sample was thus subjected to the thermal protocol displayed in Fig. 1. It has been reported that the formation of ordered solid phases in glycerol is favoured by a slow cooling to temperatures slightly above the T_g , followed by two successive isothermal treatments for triggering nucleation and crystal growth respectively. We have monitored how the crystalline nucleation influenced the dielectric response of glycerol. Selected measurements during isothermal treatment at 190 K and comparison of the spectrum at 230 K before and after such nucleation are presented in Fig. 3 and 5 respectively. During nucleation, there is a slight decrease of the permittivity. Whether this reduction is consequence of changes at the molecular level associated to crystal nucleation or simply slow geometrical adjustments of the capacitor due to mismatch of sample and spacer thermal-expansion coefficients, is hard to elucidate. Nevertheless, Fig. 3 proves the sample did not undergo any kind of crystal growth upon treatment at 190 K.

In order to demonstrate the formation of crystals seeds during the thermal treatment at 190 K, in Fig. 4 we show the kinetics of crystallization at 230 K for different conditions of nucleation. The sample non-annealed was directly cooled from room temperature to 230 K at a cooling rate of 5 K/h. The data showed in Fig. 4 indicates that the crystal growth becomes faster for longer periods of annealing at 190 K. This finding confirms the formation of crystalline nuclei at 190 K which subsequently organize into the crystal lattice at 230 K.

In Fig. 5 we show the dielectric spectrum at 230 K both before and after the nucleation process at 190 K. It is seen that the relaxation response at 230 K is almost identical before and after the treatment at 190 K. However, from the kinetics shown in Fig. 4 it is clear

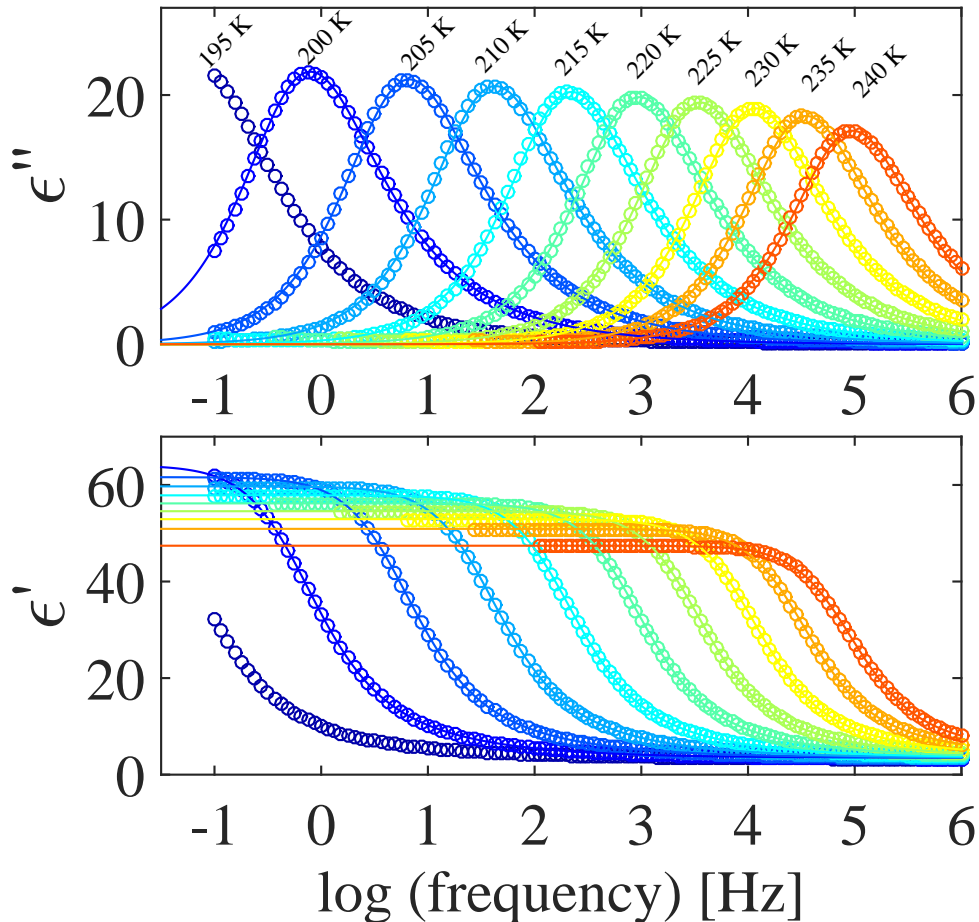


FIG. 2. Dielectric loss (top) and real part (bottom) of the complex dielectric permittivity of fully disordered supercooled glycerol at selected temperatures. Continuous lines represent the best fit of the experimental data to the EB model.

that there is in fact a structural difference between the sample before and after annealing, in one case there is (more) crystal nuclei present in the sample leading to a faster crystallization process. The fact that the two dielectric signals are identical, tells us that the formation of nuclei is a very local process which does not have any global effect on the liquid dynamics.

C. Liquid dynamics during crystal growth

With the purpose of studying the influence of crystallization on the cooperative dynamics in glycerol, frequency sweeps from 100 mHz to 1 MHz (total acquisition time 11.7 min.) were collected continuously at a constant temperature of 230 K. Selected snapshots of this real time investigation are presented in Fig. 6. The dielectric relaxation response remains unchanged during the early stages, but its intensity starts to monotonically decrease after an induction period and finally the α relaxation

peak totally vanishes. We have previously introduced $\Delta\epsilon$ as one of the factors that parametrizes Eq. 1. It is defined as the area under the dielectric relaxation curve or also as the difference between the low and high frequency plateaus of the permittivity. $\Delta\epsilon$ is extremely sensitive to changes in the fraction of mobile phase due to it is directly related to the density of fluctuating dipoles. According to the theory of dielectric relaxation and ignoring possible variations of the dipole-dipole correlations, we may consider the following proportionality

$$\Delta\epsilon \propto \frac{\mu^2 N}{k_b T} \quad (2)$$

where μ is the molecular dipole moment, k_b is the Boltzmann constant, T is the temperature and N corresponds to the total number of reorientating dipoles in the system⁸. Assuming that the transformation of a liquid substance into a crystal carries with it the corresponding reduction of fluctuating species N as molecules abandon

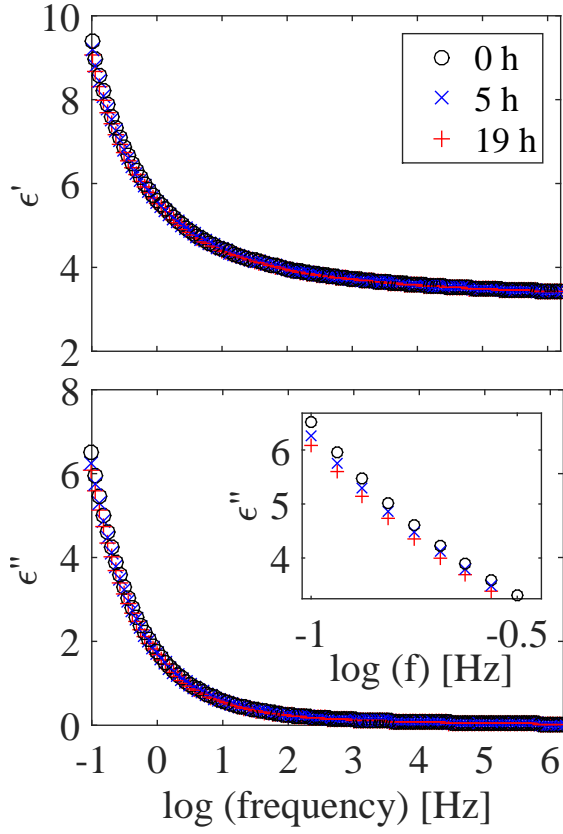


FIG. 3. Frequency dependence of the real (top) and imaginary (bottom) parts of the complex dielectric permittivity in glycerol during isothermal annealing at 190 K for times given in the top panel. The inset zooms the low frequency flank of the dielectric loss for a more detailed examination.

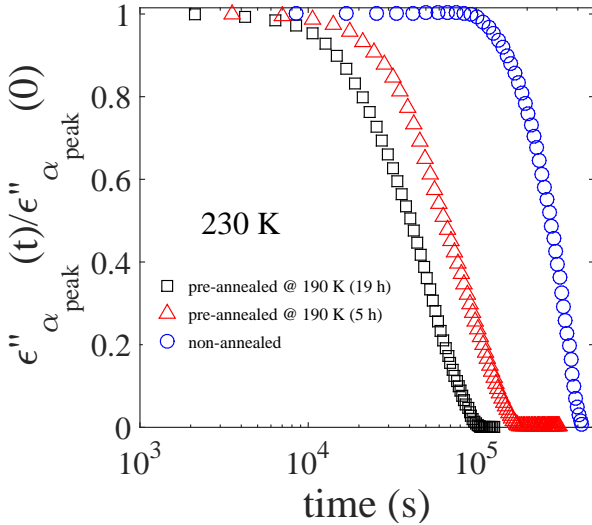


FIG. 4. Time evolution of the maximum intensity of the loss peak upon crystallization at 230 K for samples annealed at 190 K during 19 h (□), annealed 5 h at 190 K (△) and non-annealed (○). Data are normalized to the initial value.

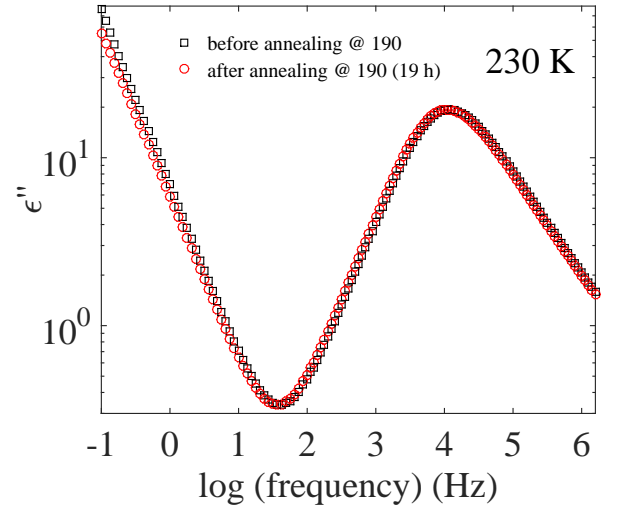


FIG. 5. Dielectric spectra of glycerol collected at 230 K, first by cooling from room temperature (□) and second after annealing at 190 K and subsequent warming up (○).

the disordered phase and attach to the surface of growing crystals where molecules become translational and rotationally immobile, one accordingly expect a depletion of $\Delta\epsilon$ via Eq. 2. This effect is clearly observed in both components of the complex permittivity as displayed in Fig. 6. The low frequency dispersion detected in $\epsilon''(\omega)$, which is assigned to pure ohmic conduction, decreases approximately at the same rate as the α relaxation peak. A reduction of the dc conductivity upon crystallization is in agreement with arguments that inversely correlate the conduction of free charges with the viscosity of the medium⁴⁰. Apart from the total extinction of the structural relaxation when the crystallization ended, it is important to remark that the location of the peak remained unchanged during the whole process, suggesting that the intrinsic nature of the structural relaxation of glycerol remains unaltered in the course of crystallization. A more detailed investigation of the temperature-dependence of the kinetics of crystallization has also been carried out and it will be the subject of a future publication⁴¹ where we also consider possible Maxwell-Wagner-type⁴² effects on the dielectric signal.

D. Liquid dynamics after aborted crystallization

We explored the crystallization of glycerol at different temperatures several times and only in one single case, the ordering process did not proceed to the end and a small fraction of liquid phase got trapped between the crystalline domains. To illustrate this aborted crystallization, Fig. 7(top) shows the evolution of the α relaxation as a function of crystallization time. Contrary to the data set shown in Fig. 6, in Fig. 7(top) a residual and stable α peak is still detected once the transi-

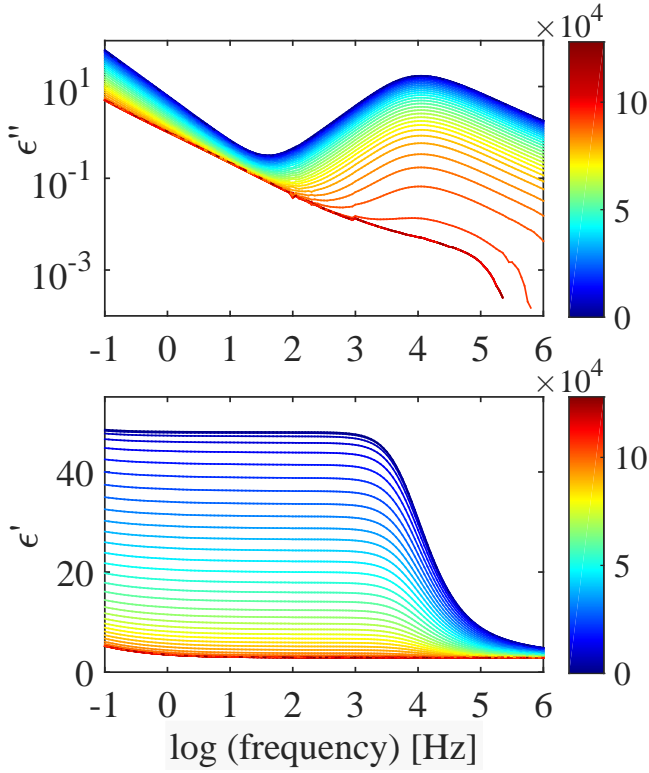


FIG. 6. Complex dielectric permittivity of supercooled glycerol upon crystallization at 230 K. Dielectric loss (top) and real part of the permittivity (bottom) are represented as a function of frequency at different stages of crystallization. Colorbars indicate the crystallization time in seconds.

tion terminates. Such coexistence between crystallites and disordered domains giving rise to an α peak is a well-known and general phenomenon in the field of semi-crystalline polymers¹¹. Here, the stability of this residual relaxation was confirmed during more than 24 hours, without any indication of loosing intensity, broadening or shifting in frequency. As a first approach, it is plausible to state that the existence of a residual relaxation, extremely weak though, implies that the crystalline growth was frustrated at the late stages. As a result, an small part of the sample ($\sim 1\%$) still in the liquid state is confined by the more rigid crystalline domains.

The kinetics of crystallization was evaluated by calculating the fraction of phase transformation as a function of time. The volume fraction of the new phase at different crystallization times $N(t)$ was estimated from the maximum intensity of the loss peak by means of the following expression:

$$N(t) = \frac{\varepsilon''_{\alpha_{peak}}(0) - \varepsilon''_{\alpha_{peak}}(t)}{\varepsilon''_{\alpha_{peak}}(0) - \varepsilon''_{\alpha_{peak}}(\infty)} \quad (3)$$

where $\varepsilon''_{\alpha_{peak}}(0)$ is the value of the dielectric loss at the frequency where the α peak is located for the pure liq-

uid, $\varepsilon''_{\alpha_{peak}}(t)$ takes the corresponding values at different crystallization times and $\varepsilon''_{\alpha_{peak}}(\infty)$ corresponds to the value of the dielectric loss at the dielectric-loss frequency for the pure crystal. For the specific case where the crystallization stopped and the exact value of $\varepsilon''_{\alpha_{peak}}(\infty)$ is unknown, we assume the same ratio between $\varepsilon''_{\alpha_{peak}}(0)$ and $\varepsilon''_{\alpha_{peak}}(\infty)$ obtained for the data at 230 K showed in Fig. 6.

Figure 7 (bottom) shows the time evolution of $N(t)$ during isothermal treatment at 230 K for the complete (\square) and aborted (\circ) phase transformations. In both cases, the data follow a sigmoidal fashion in accordance with previous studies on crystalline growth³¹. In general terms, the kinetics of the transition is quite similar and one only detects significant differences close to the end where the maximum value of the volume fraction of the new phase does not reach 1 in one of the cases.

In order to elucidate the dynamic properties of the liquid phase in the frustrated crystal, the sample described in Fig. 7(top) was subsequently cooled down to temperatures just above the T_g , collecting isothermally every 5 K the frequency dependence of the complex permittivity.

From a qualitative point of view, the temperature evolution of the α relaxation shows a similar behaviour as that for the fully disordered liquid, as shown in Fig. 8. It is worthy to remark the thermodynamic stability of the liquid phase responsible of this relaxation, as indicated by the absence of any significant drop in intensity during the temperature scan. As we did for the pure liquid, full lines in Fig. 8 correspond to the fit of the experimental data to the EB or α -circuit model (Eq. 1). In both cases, the values of α were set to 0.5 for the whole temperature range. Since we were just interested on the α peak, the slight increase of dispersion at the high frequency flank of the α peak, the so-called excess wing, was not taken into consideration⁷.

A close comparison of the fitting parameters of Eq. 1 for the liquid and aborted crystalline samples is shown in Fig. 9. The relaxation strength against temperature (panels *a* and *b*) shows a similar trend in both cases, decreasing when temperature goes up in accordance with Eq. 2. Regarding the broadening parameter k_α , Fig. 9(c) presents a similar behaviour for both kind of liquids. The values of k_α increase when temperature decreases which indicates a broader width of the distribution of relaxation times when approaching the T_g ⁷. The values of k_α account for the departure of the relaxation width from the simplest Debye model, in such a way that large values of k_α will lead to a less Debye-like relaxation^{38,43}. For the frustrated crystal one may observe slightly higher values. It is tempting to correlate this increase of k_α with a more heterogeneous landscape. However, the difference is not very prominent and we have to take into consideration that the amplitude of the relaxation for the frustrated crystal is very low meaning that the curve shape is also determined with less precision.

In Fig. 9(d) we have plotted the characteristic relax-

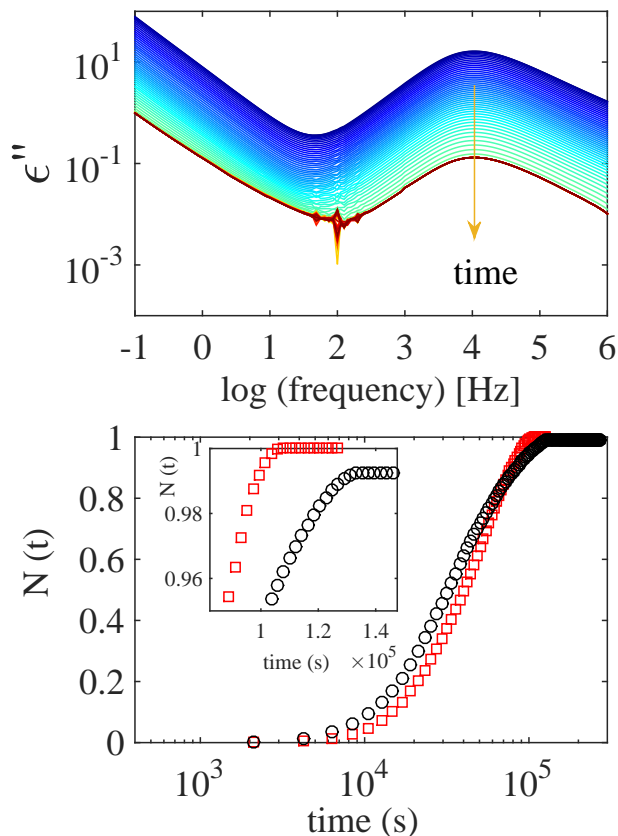


FIG. 7. (Top) Dielectric loss in logarithmic scale of the α relaxation as a function of frequency at different crystallization times during isothermal annealing at 230 K. Snapshots are shown every 3.5×10^3 s during a total crystallization time of 2.7×10^5 s. (Bottom) Time dependence of the crystalline volume fraction at 230 K for the complete (\square) and aborted (\circ) crystallization processes. The inset zooms the late stages to highlight the frustrated crystallization shown in the top panel.

ation times of the α process in the Arrhenius representation. As expected, the temperature dependence of the α relaxation times deviate from linearity as temperature goes down. For both types of liquid glycerol, the values of τ_α can be described by the empirical Vogel-Fulcher-Tammann (VFT) relation:

$$\tau_\alpha = \tau_0 \exp\left(\frac{DT_0}{T - T_0}\right) \quad (4)$$

where τ_0 is a pre-exponential factor with phonon-like time scales, D is a strength parameter related to the dynamic fragility through the following expression $m=16+590/D$ and T_0 is the Vogel temperature ($T_0 < T_g$)⁴⁴. Leaving aside the physical meaning of the parameters in Eq. 4 (see eg.⁴⁵ for a discussion), the usefulness of the VFT law for interpolating experimental points and quantifying the steepness of the relaxation plot is widely accepted^{1,2,4,45}. Solid lines in Fig. 9(d) correspond to the fits of the data to the VFT equation for the pure liq-

TABLE I. VFT parameters of the α process for the pure liquid and for the remaining liquid fraction embedded in the frustrated crystal.

VFT Parameter	Pure Liquid	Frustrated Crystal
$\log \tau_0$ (s)	-14.8	-14.9
D	18.3	18.6
T_0 (K)	128	128

uid and frustrated crystalline samples. For consistency, the relaxation times for the two kinds of liquids were fitted in the same temperature range (200-230 K). Both the data and the VFT lines practically overlap, which indicates that the nature of the α relaxation dynamics is not significantly altered by the presence of crystals. Similar values of the VFT parameters to those collected here in Table I have been reported in the literature^{7,46}.

IV. DISCUSSION

We have explored the formation of solid structures in real time in a well-known glass former glycerol. The solidification was induced by a two-step annealing procedure as suggested before^{28,29}. Our dielectric data reveal that liquid glycerol, through a nucleation step at 190 K and subsequent crystal growth at 230 K, transforms into a new phase. In most cases (not all of them shown here⁴¹), we have found a total disappearance of the α relaxation, a fact which suggests that glycerol transforms into the standard orthorhombic crystalline phase²⁵. It is worthy to remark that from dielectric relaxation data is not possible to extract direct information about the microscopic structure of the relaxing medium. Thus, our assumption that the new phase formed during the experiment described in Fig. 6 is purely crystalline, is based on the hypothesis that the formation of a glacial phase should have presumably terminated with an active relaxation. Our reasoning is in agreement with recent neutron diffraction measurements where the crystalline nature of this solid phase was unequivocally evidenced²⁹. Unfortunately, these authors could not conduct to the end the measurements at the lowest temperatures due to limited beam-time, resulting in diffraction patterns where weak crystalline reflections were superimposed to the amorphous halo. These heterogeneous diffraction patterns, despite they were probably the result of an unfinished slow kinetics, opened the possibility to speculate with the formation of nano-crystals dispersed in a disordered liquid phase^{19,28,29}. The fact that in one of the samples studied here (Fig. 7), the end of the crystallization was suddenly aborted could explain those results which speculated with the formation of a glacial phase where metastable nano-crystals are embedded in a liquid matrix^{19,28,29}. Our data just show an unfinished ordering process that resulted in a small fraction of sample remaining in the liquid state. Unlike in polymeric ma-

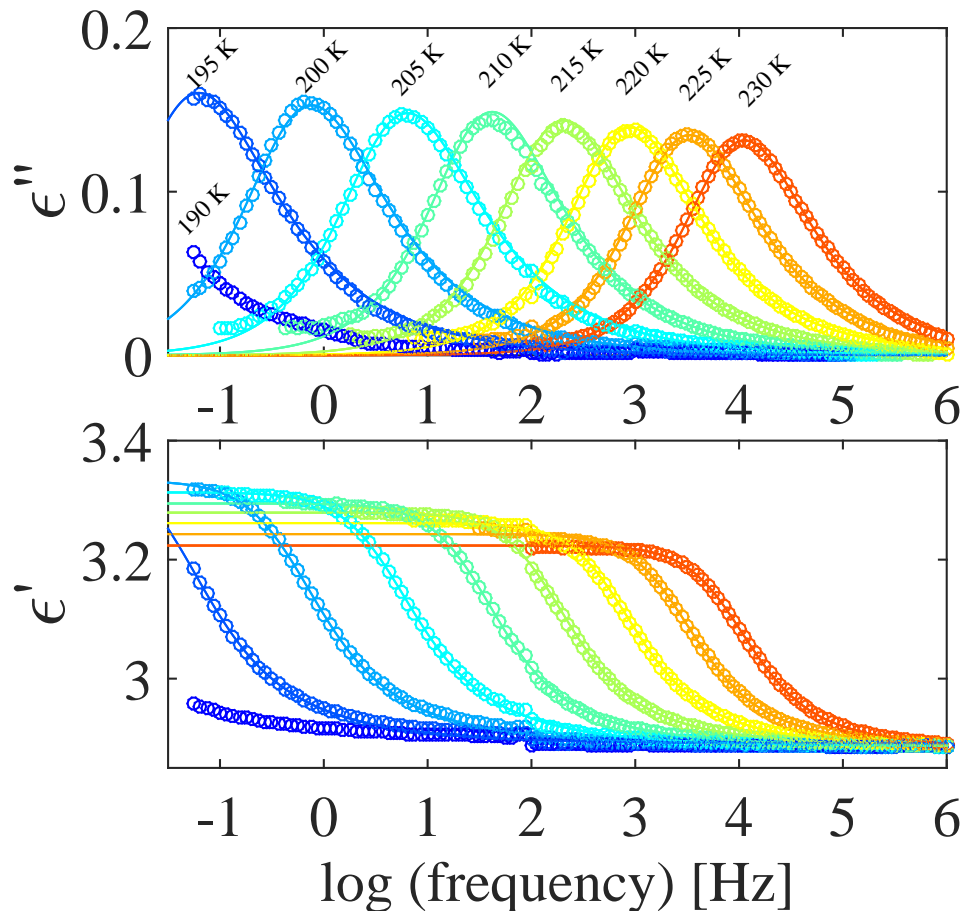


FIG. 8. Dielectric spectra of residual liquid glycerol in a frustrated crystalline phase at the labelled temperatures. Continuous lines represent the best fit of the experimental data to the EB model. Dielectric loss (top) and real part (bottom) of the complex dielectric permittivity are represented as a function of frequency.

terials where the formation of semi-crystalline structures is a common feature, few examples can be found in the literature where a low molecular weight liquid does not crystallize into a 100 % crystallinity system³¹.

We have evidenced that the nature of the α relaxation dynamics does not suffer important modifications during crystallization. We have extended our study along the whole crystallization process, from a well controlled nucleation step to the crystal growth. Interestingly, the structural relaxation remained unaffected, first by the density fluctuations that trigger the formation of nuclei, and second during the thickening of the lattice structure.

Taking advantage to the aborted crystallization that took place in one of the studied samples, we could explore the temperature evolution of the α relaxation associated to a small fraction of liquid phase surrounded by the crystalline network. Our results indicate that the dynamics remained virtually identical to the bulk liquid in terms of location of the α peak, spectral shape and activation energy. A relaxation process in crystalline glycerol was reported by Ryabov *et al.*⁴⁷, where a sample of dry glycerol was crystallized on heating, giving as a result a new

dielectric mode five orders of magnitude slower than the α process for the pure liquid. This new mode exhibited an Arrhenius behaviour, similar to other dielectric relaxation processes detected in molecular crystals^{48,49} and it was assigned by the authors to either defects in the crystalline lattice or to the presence of disordered domains located at the interface between crystalline grains. In contrast to the observation by Ryabov *et al.*⁴⁷, here we detect a relaxation with the same features to the one showed by the pure liquid, in such a way that we may confirm that it does not correspond to the relaxation of crystalline glycerol itself, but to a kind of metastable semi-crystalline system. We do not see any evidence of the slow mode reported by Ryabov *et al.*⁴⁷.

Several factors have been proposed to affect the mobility of the liquid at the proximities of the crystal/liquid interface during crystallization, including the existence of pre-ordered configurations and the different ability of the molecules to be accommodated on the surface of the growing lattice. In the latter case, it is expected that not all molecules near the crystal/liquid interface show the same geometrical preferences to attach to the crystal.

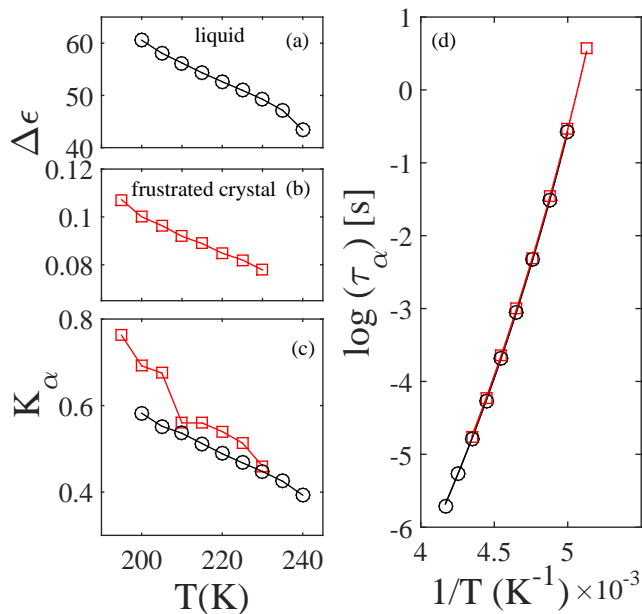


FIG. 9. Temperature dependence of the fitting parameters of the EB model (Eq. 1) for the pure liquid (\circ) and frustrated crystalline glycerol (\square). Panels *a* and *b* display the dielectric strength $\Delta\epsilon$ and panel *c* the broadening parameter k_α . In panel *d* we show the characteristic relaxation times of the α process with reciprocal temperature. Solid lines in *d* are fits to the VFT equation. Lines in *a*, *b* and *c* are guides to the eye.

For both cases, the activation energy that governs the short distance diffusion may increase as compared to the pure liquid³¹. Here we report that glycerol, at least for the time scale detected by dielectric spectroscopy, does not present variations in its mobility upon crystallization. The molecules in crystalline glycerol are in an extended conformation in which the two dihedral angles defined by the intersection between two specified planes within the molecule are situated in a range of 120° and 240° ²⁵. On the contrary, Towey et al.²⁴ have recently reported that in the liquid state the most probable conformer shows a less extended structure where the second dihedral an-

gle presents values in the range 240 - 360° . Therefore, the transference of units from the liquid on to the surface of the growing crystal should imply, at least for an important fraction of molecules, the necessity of conformational transitions to the extended or coplanar configuration. However, according to our data, this does not cause any global effect on the dynamics. The lack of dynamical signature of the crystallization process indicates that the changes in the H-bond network as well as the conformational changes taken place during the crystallization are very local. Thus, very few molecules at the phase boundary are changing structure while the majority of the molecules are either in the crystal or in the ordinary bulk liquid.

V. CONCLUSIONS

We present, to the best of our knowledge, the first study in real time in the isothermal crystallization of glycerol by using dielectric spectroscopy. We demonstrate that liquid glycerol transforms into a crystalline material by following a two-step nucleation and crystal growth protocol. Our results do not support the formation of a distinct solid phase from the standard crystalline lattice. We have also shown that in one of the samples studied, the starting liquid transformed into an incomplete crystalline phase with a residual liquid fraction. For a period of more than one day we proved the metastability of this frustrated crystal. The dynamics of this remaining liquid phase was studied as a function of temperature showing features very close to the pure liquid material. In addition to that, we have evidenced that during the ordering process the α relaxation dynamics remains unaltered, revealing that neither the nucleation period nor the crystal growth affected the nature of the cooperative motions in supercooled glycerol.

ACKNOWLEDGMENTS

This work has been funded by the Danish Council for Independent Research (Sapere Aude: Starting Grant). Technical support from the workshop at IMFUFA (Department of Science and Environment, Roskilde University) is also acknowledged.

* asanz@ruc.dk

¹ P. Debenedetti and F. Stillinger, *Nature* **410**, 259 (2001).

² L. Berthier and G. Biroli, *Reviews of Modern Physics* **83**, 587 (2011).

³ L. Berthier and M. D. Ediger, *Physics Today* **69**, 40 (2016).

⁴ M. Ediger, C. Angell, and S. Nagel, *Journal of Physical Chemistry* **100**, 13200 (1996).

⁵ J. C. Dyre, *Journal of Physics: Condensed Matter* **19**, 205105 (2007).

⁶ B. Jakobsen, C. Maggi, T. Christensen, and J. C. Dyre, *Journal of Chemical Physics* **129**, 184502 (2008).

⁷ P. Lunkenheimer and A. Loidl, *Chemical Physics* **284**, 205 (2002).

⁸ A. Schönhalz and F. Kremer, *Broadband Dielectric Spectroscopy*, Springer-Verlag Berlin Heidelberg (2003).

⁹ P. Sillren, A. Matic, M. Karlsson, M. Koza, M. Maccarini, P. Fouquet, M. Goetz, T. Bauer, R. Gulich, P. Lunkenheimer, A. Loidl, J. Mattsson, C. Gainaru, E. Vynokur, S. Schildmann, S. Bauer, and R. Böhmer, *Journal of Chemical Physics* **140**, 124501 (2014).

¹⁰ M. Paluch, M. Sekula, S. Pawlus, S. Rzoska, J. Ziolo, and C. Roland, *Physical Review Letters* **90**, 175702 (2003).

- ¹¹ A. Nogales, Z. Denchev, I. Sics, and T. Ezquerra, *Macromolecules* **33**, 9367 (2000).
- ¹² K. Murata and H. Tanaka, *Nature Materials* **11**, 436 (2012).
- ¹³ P. Lunkenheimer, R. Wehn, and A. Loidl, *Journal of Non-Crystalline Solids* **352**, 4941 (2006).
- ¹⁴ J. Martin, C. Mijangos, A. Sanz, T. A. Ezquerra, and A. Nogales, *Macromolecules* **42**, 5395 (2009).
- ¹⁵ M. Arndt, R. Stannarius, H. Groothues, E. Hempel, and F. Kremer, *Physical Review Letters* **79**, 2077 (1997).
- ¹⁶ J. Wuttke, J. Hernandez, G. Li, G. Coddens, H. Z. Cummins, F. Fujara, W. Petry, and H. Sillescu, *Physical Review Letters* **72**, 3052 (1994).
- ¹⁷ P. Lunkenheimer, A. Pimenov, M. Dressel, Y. Goncharov, R. Bömer, and A. Loidl, *Physical Review Letters* **77**, 318 (1996).
- ¹⁸ K. Schröter and E. Donth, *The Journal of Chemical Physics* **113**, 9101 (2000).
- ¹⁹ R. Zondervan, T. Xia, H. van der Meer, C. Storm, F. Kulzer, W. van Saarloos, and M. Orrit, *Proceedings of the National Academy of Sciences of the United States of America* **105**, 4993 (2008).
- ²⁰ Y. Hayashi, A. Puzenko, and Y. Feldman, *Journal of Non-Crystalline Solids* **352**, 4696 (2006).
- ²¹ L. A. Roed, D. Gundermann, J. C. Dyre, and K. Niss, *Journal of Chemical Physics* **139**, 01101 (2013).
- ²² G. J. Cuello, F. J. Bermejo, R. Fayos, R. Fernández-Perea, A. Criado, F. Trouw, C. Tam, H. Schober, E. Enciso, and N. G. Almarza, *Physical Review B* **57**, 8254 (1998).
- ²³ A. V. Egorov, A. P. Lyubartsev, and A. Laaksonen, *Journal of Physical Chemistry B* **115**, 14572 (2011).
- ²⁴ J. J. Towey, A. K. Soper, and L. Dougan, *Physical Chemistry Chemical Physics* **13**, 9397 (2011).
- ²⁵ F. J. Bermejo, A. Criado, A. de Andres, E. Enciso, and H. Schober, *Physical Review B* **53**, 5259 (1996).
- ²⁶ C. Talon, Q. Zou, M. Ramos, R. Villar, and S. Vieira, *Physical Review B* **65**, 012203 (2002).
- ²⁷ U. Buchenau, R. Zorn, and M. A. Ramos, *Physical Review E* **90**, 042312 (2014).
- ²⁸ M. E. Möbius, T. Xia, W. van Saarloos, M. Orrit, and M. van Hecke, *The Journal of Physical Chemistry B* **114**, 7439 (2010).
- ²⁹ H.-F. Yuan, T. Xia, M. Plazanet, B. Dem, and M. Orrit, *Journal of Chemical Physics* **136**, 041102 (2012).
- ³⁰ A. Ha, I. Cohen, X. Zhao, M. Lee, and D. Kivelson, *The Journal of Physical Chemistry* **100**, 1 (1996).
- ³¹ M. Descamps and E. Dudognon, *Journal of Pharmaceutical Sciences* **103**, 2615 (2014).
- ³² K. Adrjanowicz, K. Kaminski, M. Paluch, and K. Niss, *Crystal Growth & Design* **15**, 3257 (2015).
- ³³ P. Tripathi, M. Romanini, J. L. Tamarit, and R. Macovez, *International Journal of Pharmaceutics* **495**, 420 (2015).
- ³⁴ A. Sanz, M. Jimenez-Ruiz, A. Nogales, D. Marero, and T. Ezquerra, *Physical Review Letters* **93**, 015503 (2004).
- ³⁵ J. Dobberty, J. Hannemann, C. Schick, M. Ptter, and H. Dehne, *The Journal of Chemical Physics* **108**, 9062 (1998).
- ³⁶ B. Igarashi, T. Christensen, E. H. Larsen, N. B. Olsen, I. H. Pedersen, T. Rasmussen, and J. C. Dyre, *Review of Scientific Instruments* **79**, 045106 (2008).
- ³⁷ B. Igarashi, T. Christensen, E. H. Larsen, N. B. Olsen, I. H. Pedersen, T. Rasmussen, and J. C. Dyre, *Review of Scientific Instruments* **79**, 045105 (2008).
- ³⁸ N. Sağlanmak, A. I. Nielsen, N. B. Olsen, J. C. Dyre, and K. Niss, *The Journal of Chemical Physics* **132**, 024503 (2010).
- ³⁹ It is well documented that the dielectric loss of the α relaxation of viscous molecular liquids at the high frequency limit shows a power law dependence of $\omega^{-\alpha}$, where α normally takes values of 0.5 when temperature approaches the glass transition.
- ⁴⁰ C. M. Roland, S. Hensel-Bielowka, M. Paluch, and R. Casalini, *Reports on Progress in Physics* **68**, 1405 (2005).
- ⁴¹ A. Sanz and K. Niss, In preparation.
- ⁴² M. H. Jensen, C. Alba-Simionesco, K. Niss, and T. Hecksher, *The Journal of Chemical Physics* **143**, 134501 (2015).
- ⁴³ P. Debye and H. Falkenhagen, *Physikalische Zeitschrift* **29**, 401 (1928).
- ⁴⁴ R. Böhmer, K. L. Ngai, C. A. Angell, and D. J. Plazek, *The Journal of Chemical Physics* **99**, 4201 (1993).
- ⁴⁵ T. Hecksher, A. I. Nielsen, N. B. Olsen, and J. C. Dyre, *Nature Physics* **4**, 737 (2008).
- ⁴⁶ S. Sudo, M. Shimomura, N. Shinyashiki, and S. Yagihara, *Journal of Non-Crystalline Solids* **307-310**, 356 (2002).
- ⁴⁷ Y. Ryabov, Y. Hayashi, A. Gutina, and Y. Feldman, *Physical Review B* **69**, 189904 (2004).
- ⁴⁸ A. Sanz, D. Rueda, A. Nogales, M. Jimenez-Ruiz, and T. Ezquerra, *Physica B: Condensed Matter* **370**, 22 (2005).
- ⁴⁹ K. Amann-Winkel, C. Gainaru, P. H. Handle, M. Seidl, H. Nelson, R. Böhmer, and T. Loerting, *Proceedings of the National Academy of Sciences of the United States of America* **110**, 17720 (2013).